Spectral-Efficient Aircraft Pairing for Massive MIMO NOMA in Aeronautical Communication

Amir K. Hanna*, Ahmed M. Abd El-Haleem, and Ihab A. Ali

Electronics and Communication Engineering Department, Helwan University, Cairo, Egypt
Email: amirkhairat34@gmail.com (A.K.H.); ahmed_abdelkhaliq@h-eng.helwan.edu.eg (A.M.A.E-H.); ehab_ali02@h-eng.helwan.edu.eg (I.A.A.)
*Corresponding author

***Abstract*—As air traffic volumes rise, enhancing the spectral efficiency of aeronautical communication systems is crucial. International Civil Aviation Organization (ICAO) proposes using the L-Band Digital Aeronautical Communication System (LDACS) to meet future demands, but its implementation faces legal and interference challenges with existing L-band systems like Joint Tactical Information Distribution System (JTIDS), Military Tactical Air Navigation (TACAN), and Distance Measurement Equipment (DME). To address this, we propose employing Non-Orthogonal Multiple Access (NOMA) in Very High Frequency (VHF) digital systems, aiming to boost capacity without introducing new bands. Our study focuses on maximizing spectral efficiency using NOMA-based massive Multi-Input Multi-Output (mMIMO) for aeronautical communications. We evaluate different pairing algorithms (Gale Shapley, Hungarian, and correlation-based) and beamforming techniques Zero Forcing and Maximum Ratio (ZF and MR), finding that GS pairing with ZF beamforming yields the optimal solution. Results show that all three algorithms outperform fixed pairing NOMA, with GS being the least complex, followed by Hungarian and correlation-based. Additionally, ZF beamforming outperforms MR in achieving spectral efficiency. This integrated approach offers a promising strategy for enhancing aeronautical communication systems amidst growing air traffic demands.**

***Keywords*—aeronautical communications, air traffic Control, non-orthogonal multiple access, Massive Multi-Input Multi-Output (mMIMO), pairing algorithms**

I. Introduction

Analog voice communications between Air Traffic Control (ATC) on the ground station and the pilots onboard the aircraft are used as Air/Ground (A/G) communication and a Very High Frequency (VH)F data link for data transmission, or both digitally on a VHF digital link; all VHF digital links are shown in Table I. The Very High Frequency (VHF) band is sporadically used for A/G, such as during the flight's backup phases when a pilot communicates with ground-based ATC [1–5].

Manuscript received October 26, 2023; revised January 27, 2024; accepted February 1, 2024; published June 3, 2024.

TABLE I. VHF Data Links [4]

Name	ACARS*	VDL Mode-2	VDL Mode-3	VDL Mode-4
Access Method	Non-Persistent CSMA	CSMA	TDMA	STDMA
Capability	Data Only	Data Only	Data and Voice	Data Only
Modulation	MSK	D8PSK	D8PSK	GFSK
Channel bandwidth	25 kHz	25 kHz	25 kHz	25 kHz
Data Rate	3.4 kbps	31.5 kbps	31.5 kbps	19.2 kbps

Aircraft Communications Addressing and Reporting System *

The VHF band's frequency resources for aeronautical Air Traffic Management (ATM) communications are no longer sufficient to keep up with the current surge in air traffic [6]. By 2025, the number of airspace regions will have reached their maximum growth rate [2]. Moreover, the requirements for higher data rates in aeronautical radio communication systems to serve different applications are currently increasing. As a result, more than the facilities the current VHF resources may deliver may be needed to meet the growing needs for A/G communications [3]. So, to address this issue, International Civil Aviation Organization (ICAO) considered using L-band for aeronautical communication [1–3], but the use of this band will impact the legal systems that work in this band, such as Distance Measuring Equipment (DME), the Military Tactical air Navigation (TACAN) system, and the Joint Tactical Information Distribution System (JTIDS) [7]. As a result, prior studies aimed to examine possible solutions to address this problem, such as the LDACS I system based on OFDM and the LDACS II based on GSM. The results of the study in Ref. [8] demonstrate that FBMC has superior performance (and spectral containment) than the L-DACS schemes. The work also presented a FBMC-based communication system and outlined its advantages over the LDACS system. A Cognitive Radio (CR) network with simultaneous primary DME channels is suggested in Ref. [9] to enable effective spectrum utilization. Utilizing an adaptive threshold Distance Measuring Equipment (DME) energy detector in the LDACSI-CR network, the suggested spectrum sensing technique achieves the best balance between false alarm detection and DME signal identification. Based on the properties of DME pulse signals in Ref. [10], an adaptive threshold energy detection

spectrum sensing approach is proposed. All the previous works we have mentioned aimed to present solutions for resolving the interference problem between LDACS and existing systems. In our proposed solution, we investigate the utilization of the VHF band with the new access technique, NOMA. Our work focused on the spectral-efficient aircraft pairing-based massive MIMO NOMA for aeronautical communication. We can summarize our contributions to this research as the following:

- Enhance the spectral efficiency of aeronautical communication by employing massive MIMO NOMA.
- Compare the spectral efficiency enhancement between three different pairing Algorithms (GS, Hungarian, and correlation-based) and the fixed pairing algorithm.
- Compare the complexity of GS, Hungarian, and correlation-based algorithms.
- Compare the Spectral Efficiency (SE) with the Zero Forcing (ZF) Maximal Ratio (MR) beamforming algorithms.

The rest of the paper is organized as follows: Section II presents a system model for aeronautical communication based on massive MIMO NOMA. Section III presents the results and discussion. Finally, Section IV is the conclusion.

II. System Model

Assume a single-cell system with a Control Tower Ground Station (CTGS) equipped with M antennas (where M >> N), serving aircrafts. Each aircraft has a single antenna. The served aircrafts can be divided into two equivalent groups. The first group includes the cell-Center Aircraft (CA), while the second group comprises the cell-Edge Aircraft (EA), as illustrated in Fig. 1.

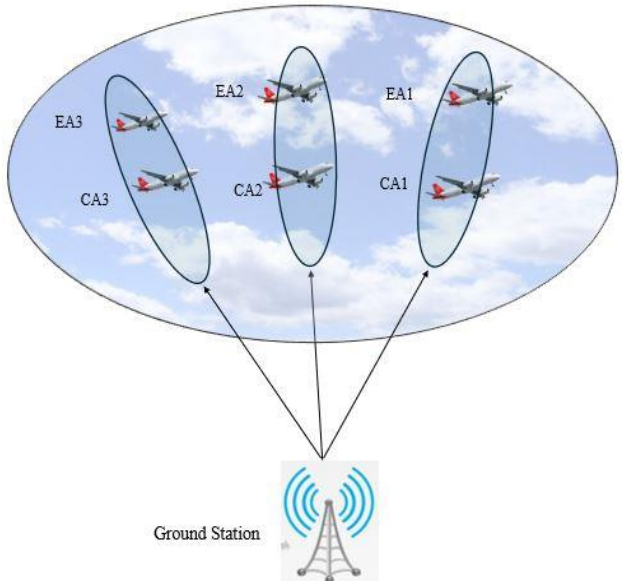

Fig. 1. Aeronautical communication based on massive MIMO NOMA.

A. Description of Aircraft as Downlink Channel Vector

$$q_a = \sqrt{\beta_a}\, h_a \qquad \forall \ a = 1 \ldots, N \tag{1}$$

where: q_a is the downlink channel vector.

β_a is the large-scale fading coefficient, which just considers the path-loss component and leaves out the impact of shadowing.

The vector h_a presents an arbitrary constant or deterministic vector, and its values are perfectly known at the base station CTGS. This is possible because deterministic variables can be estimated with minimal estimation overhead. In other words, the CTGS has accurate knowledge of the values of h_a, as estimating these deterministic variables doesn't require a significant computational burden [11, 12].

In the case of a Uniform Linear Array (ULA) the channel vector will be:

$$\boldsymbol{h}_a = \left[1\ e^{j2\pi\frac{d}{\lambda}sin\,\varphi_a}, \ldots\ldots\ldots, \ e^{j2\pi\frac{d}{\lambda}sin\,\varphi_a\,(M-1)}\right]^T \tag{2}$$

where: d stands for the ULA's separation of two neighboring antennas, the carrier wavelength is λ, and φ_a is the angle at which the CTGS station departs from the a^{th} aircraft in relation to the array boresight.

It's crucial to emphasize that in the Line of Sight (LOS) scenario, we adopt the assumption of a Uniform linear Array (ULA). Eq. (2) remains valid under the condition that users are positioned in the far field of the ULA, and there is no presence of scattering [12].

The aircraft received a downlink signal provided by the vector y_a [12]:

$$y_a = \sum_{i=1}^{N} q_a^T\, s_i + n_a \tag{3}$$

where s_i is the aircraft's beamformed data symbol and n_a ~ CN (0, 1) is the additive noise.

$$s_a = w_a \sqrt{p_a}\, z_a \tag{4}$$

Here, the data symbol for aircraft a is presented by z_a ~ CN (0,1) (CN means complex normal distribution), the normalized transmission power is presented by p_a, and the normalized beamforming vector for aircraft a is presented by w_a, where E $\{\|w_a\|^2\}$ = 1.

Therefore, we can modify Eq. (3).

$$y_a = \sqrt{\beta_a}\, h_a^T \sum_{i=1}^{N} w_i \sqrt{p_i}\, z_i + n_a \tag{5}$$

$$\sqrt{\beta_a\, p_a}\, h_a^T\, w_a\, z_a + \sqrt{\beta_a} h_a^T \sum_{\substack{i=1,\\ i\neq a}}^{N} w_i \sqrt{p_i}\, z_i + n_a \tag{6}$$

where p_a is the transmitted power for aircraft a and $n_a \sim \mathrm{CN}(0,1)$ is the AWGN. Assume that the data symbol for aircraft a is $z_a \sim \mathrm{CN}(0,1)$.

B. Beamforming Vectors

There are different beamforming techniques, like Zero-Forcing (ZF), Minimum Mean Square Error (MMSE), and Maximum Ratio (MR) [13, 14]. We used Zero-Forcing (ZF) and Maximum Ratio (MR) beamforming schemes in our work. The ZF beamforming technique performs well in eliminating inter-user interference even in the case of imperfect Channel State Information (CSI), where residual interference exists. The beamforming matrix V = $[\boldsymbol{v}_1\ ;\ \boldsymbol{v}_2\ ;\ \ldots, \boldsymbol{v}_N\ ]$ is given by:

$$V = H((H)^H H)^{-1} \tag{7}$$

where: $H = [h_1 ; h_2 ; \dots , h_N]$ is the matrix of the channel. The ZF beamforming vector w_a for aircraft a for the LOS scenario is given by:

$$w_a = \frac{V_a}{\|V_a\|} \quad (8)$$

The MR beamforming technique is one of the typical techniques that increases SNR. It proves effective in MU-MIMO scenarios, particularly when the base station emits weak signals to the users. The MR beamforming vector w_a for aircraft a for the LOS scenario is given by:

$$V = (H)^H \quad (9)$$

$$w_a = \frac{V_a}{\|V_a\|} \quad (10)$$

C. Spectral Efficiency Calculation for LOS Scenario

Click or tap here to enter text.

The achievable rate for the aircraft a is [12]:

$$SE_a^{NOMA} = log_2\left(1 + \frac{p_a \beta_a |h_a^T w_a|^2}{\beta_a \sum_{\substack{i \neq a \\ i \neq cea}}^{N} p_i |h_a^T w_i|^2 + 1}\right), \forall \text{ a } \in \text{CA} \quad (11)$$

$$SE_a^{NOMA} = log_2\left(1 + \frac{p_a \beta_a |h_a^T w_a|^2}{\beta_a \sum_{i \neq a}^{N} p_i |h_a^T w_i|^2 + 1}\right), \forall \text{ a } \in \text{EA} \quad (12)$$

D. Aircraft Pairing Algorithms

There are two major groups of aircraft. The first group is made up of high-channel gain cell-center aircraft, and the second group is made up of low-channel gain cell-edge aircraft. To create a NOMA group that ensures maximal Spectral Efficiency (SE), the pairing algorithm chooses one aircraft from the cell center aircrafts and one from the cell edge aircrafts.

1) Gale-shapley algorithm

Following is the formulation of the aircraft pairing problem [15–17]:

$$Maximize \sum_{CA=1}^{\frac{N}{2}} \sum_{EA=\frac{N}{2}+1}^{N} f_{ca,ea}\, SE \quad (13)$$

where:

$$f_{ca,ea} = \begin{cases} 1, & if\ CA\ is\ aleardy\ paired\ with\ EA \\ 0, & if\ CA\ is\ not\ paired\ with\ EA \end{cases}$$

The stable marriage criteria are considered by the Gale-Shapley algorithm to find partners. In the first group, each user creates his own set of preferences for the other group members. To ensure that they approach the second group's most favored users, each member's selections in the first group are listed in descending order. Second group members are free to consent to the offer if it is available or reject it if they want to remain with their present partners. Members of the second group have the option to choose between their current partners and new proposals. Aircrafts from the first group not partnered in the first round of suggestions are asked to re-propose in the order of their list of preferences. According to Eq. (13), the preference list's values are computed. Suppose neither aircraft from the first group nor an aircraft from the second group prefers the other over their existing companions but is not matched with one another. In that case, the pairing process's outcome is stable. The outcome for the group performing proposals for the Gale-Shapley algorithm is stable. Algorithm 1 presents the Gale-Shapley algorithm. Table II introduces a sample preference list for six aircrafts.

TABLE II. THE CELL-CENTER AIRCRAFTS PREFERENCE LIST

Preferences of the First Group			
CA 1	EA 1	EA 3	EA 2
CA 2	EA 3	EA 1	EA 2
CA 3	EA 1	EA 3	EA 2

Algorithm 1: Gale-Shapley Algorithm

1st step:
Based on SE calculations, each cell-center aircraft creates a list of their preferred cell-edge aircrafts in descending order.
2nd step:
I) Every unpaired cell-center aircraft asks to be matched with the cell-edge aircraft that it values the most.
II) In response to the cell center aircraft it prefers the most, each cell-edge aircraft says "yes" and "no" to all other cell-center aircrafts. The cell-edge aircraft is thus momentarily "paired" with the cell-center aircraft that it has thus far shown the greatest liking for.
3rd step:
I) Whether or not that cell-edge aircraft is already paired, each aircraft in an unpaired cell-center sends a pairing request to his preferred cell-edge counterpart.
II) Each cell-edge user responds with a "yes" if they are not currently paired or if they find this cell-center user more preferable than their existing temporary partner. In such a scenario, the cell-edge aircraft rejects their current temporary partner, who then becomes unpaired.
4th step:
Up until everyone is partnered, this process is repeated.

2) Hungarian algorithm

The Hungarian algorithm is used to overcome the difficulty of designating a single agent for a single task [18, 19]. We provide an objective optimization matrix for SE calculations involving aircraft at the cell-center and cell edge since it is initially designed to address minimization issues, as illustrated in Table III. Choosing the pairs that maximize SE is the goal right now. The objective matrix for optimization is modified and transformed into the cost matrix to turn the optimization problem into a minimization problem. As indicated in Table IV, the modification procedure begins by determining the most significant value in each column, after which all column elements are deducted from their respective largest values. The cost matrix that must be minimized is the resulting matrix. The optimization objective matrix is maximized when the cost matrix is minimized. Algorithm 2 provides a summary of the Hungarian algorithm. The following formulation represents the optimization problem:

$$Minimize \sum_{CA=1}^{\frac{N}{2}} \sum_{EA=\frac{N}{2}+1}^{N} f_{ca,ea}\, \delta_{cost} \quad (14)$$

where:

$$f_{ca,ea} = \begin{cases} 1, & if\ CA\ is\ aleardy\ paired\ with\ EA \\ 0, & if\ CA\ is\ not\ paired\ with\ EA \end{cases}$$

TABLE III. AN ILLUSTRATION OF THE OPTIMIZATION OBJECTIVE MATRIX FOR THE HUNGARIAN ALGORITHM

	EA 1	**EA 2**	**EA 3**
CA 1	8 b/s/Hz	10 b/s/Hz	14 b/s/Hz
CA 2	8 b/s/Hz	8 b/s/Hz	16 b/s/Hz
CA 3	12 b/s/Hz	13 b/s/Hz	4 b/s/Hz

TABLE IV. THE COST MATRIX TO BE MINIMIZED

	EA 1	EA 2	EA 3
CA 1	8	6	2
CA 2	8	8	0
CA 3	4	3	12

So, we can complete the algorithm steps as the following:

Each row's other values should be subtracted from the row's smallest value:

	EA 1	EA 2	EA 3
CA 1	6	4	0
CA 2	8	8	0
CA 3	1	0	9

Now, remove the smallest number in each column from all other values in the column, then draw as few lines as you can through the row and columns with 0 entries:

	EA 1	EA 2	EA 3
CA 1	5	4	0
CA 2	7	8	0
CA 3	0	0	9

Each row's other values should be subtracted from the row's smallest value:

	EA 1	EA 2	EA 3
CA 1	1	0	–4
CA 2	3	4	–4
CA 3	0	0	9

Add the following to the already-covered columns:

	EA 1	EA 2	EA 3
CA 1	1	0	0
CA 2	3	4	0
CA 3	0	0	13

We're done because there are only 3 lines. Only one 0 per row and column will be included in the assignment, which will be made where the 0s appear in the matrix.

	EA 1	EA 2	EA 3
CA 1	1	0	0
CA 2	3	4	0
CA 3	0	0	13

Algorithm 2: Change the original values to

12 + 10 + 16 = 38 b/s/Hz

1st step:

Establish a cost matrix.

2nd step:

Subtract the other elements in each row from the smallest element in each row. Continue similarly for each column.

3rd step:

Star or prime all 0s, with starred 0s designating a specific set of 0s and primed 0s designating possible prospects.

4th step:

Cover every column that contains a stared zero. If N/2 columns are covered, proceed to the "done" step; otherwise, go back to step 5.

5th step:

If there is an uncovered zero, designate it as a primed zero. Proceed to step 6 if there is no starred zero in the row that contains the newly primed zero. However, if there is a starred zero in that row, cover the row and uncover the column that contains the starred zero. Repeat this process until all zeros are covered. Save the value of the smallest uncovered element and proceed to step 7.

6th step:

Until a primed zero that doesn't have a starred zero in its column generates a succession of alternate primed and starred zeros, remove all primes, unstar all starred zeros, star all primed zeros, and reveal all lines. Go back to step 4.

7th step:

Subtract the value determined in step 5 from each element in every uncovered column and add it to each element in every covered row. Return to step 5 without making any changes to primes, stars, or covered lines.

8th step:

The cost matrix's position of highlighted zeros identifies the user pairings that maximize SE.

3) Correlation-based pairing

The comparison between cell-edge and cell-center aircraft channels serves as the foundation for this pairing [12]. After channel vector estimation, the control Tower Ground Station (CTGS) generates the correlation among the channel estimations for the Non-Line of Sight (NLOS) scenario and NOMA groupings. Correlation is calculated between the channel vectors directly for the Line of Sight (LOS) scenario. Given the strong correlation value, the beamforming vector will match both aircraft in the NOMA pair. The channels of cell center aircraft and cell edge aircraft are correlated as follows:

$$\rho_{ca,ea} = \frac{|\hat{h}_{ca}\,\hat{h}_{ea}^{H}|}{\|\hat{h}_{ca}\|\,\|\hat{h}_{ea}\|} \quad (15)$$

where:

$\rho_{ca,ea}$: is the correlation factor between the cell center aircraft channel and the cell edge aircraft channel.

$\hat{h}_{ca}$: is the cell center aircraft channel response.

$\hat{h}_{ea}$: cell edge aircraft channel response

Hat symbol if means estimated channel in case of NLOS scenario.

III. RESULT AND DISCUSSION

A. Complexity Analysis

Considering that the scenario involves N aircrafts, the GS algorithm's processing cost depends on how many repetitions are needed until convergence. The complexity calculation is $O\left(\left(\frac{N}{2}\right)^2\right)$ [20].

The number of iterations necessary to find the ideal pairs determine the complexity of the Hungarian algorithm, which is $O\left(\left(\frac{N}{2}\right)^3\right)$ [20].

The complexity of correlation computations is $O(N^2M)$ since processing complexity for norm computations and single value multiplication has been left out of the denominator. At the same time, the numerator needs to do (M) complex multiplications. The procedure is carried out (N^2) times [12].

The complexity of the pairing techniques we utilized in our research is calculated in Table V. For M = 36 CTGS antennas and N = 20 aircrafts, complexity is computed. According to the complexity analysis equations, correlation-based pairing has the highest level of complexity, followed by the Hungarian algorithm, and finally, the GS algorithm with the lowest level of complexity.

TABLE V. COMPLEXITY OF DIFFERENT PAIRING ALGORITHMS

Pairing Algorithm	Complexity
Gale Shapley	100
Hungarian	1000
Correlation- based	14400

The necessity of channel correlation must be considered in our simulation when generating channels. By reducing interference from other pairs, the strong correlation increases the weak user's rate. As a result, the correlation between users' channels emphasizes the impact of the user pairing procedure, which also helps weak aircrafts in various pairings and has a clear impact on system performance metrics. The simulation parameters employed are described in Table VI.

TABLE VI. SIMULATION PARAMETERS [21, 22]

Parameter	Value
Average CA distance	25 km
Average EA distance	75 km
CTGS antennas	36
B. W	19 MHz
Noise power spectral density	–127 dBm/Hz
Channel	LOS
Beamforming Techniques	ZF, MR
Transmitted power	50 dBm
Power allocation	CU 75% EU 25%
Pass loss exponent	2

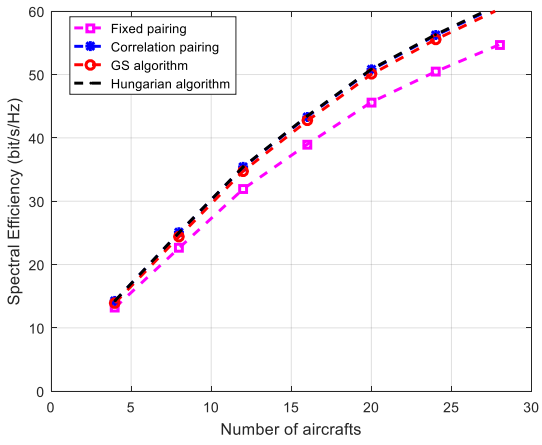

Fig. 2. Spectral efficiency versus the number of aircrafts fixed with pairing NOMA and three different pairing algorithms (GS, Hungarian, and correlation-based) with M = 36, ZF beamforming.

Fig. 2 illustrates that the GS algorithm, the Hungarian algorithm, and the correlation-based algorithm yield identical spectral efficiency. All three outperform fixed pairing, as fixed pairing selects predetermined pairs irrespective of channel conditions. In contrast, the GS algorithm, the Hungarian algorithm, and the correlation-based algorithm rely on dynamic pairing, providing flexibility and adaptability. This dynamic approach optimizes pairings based on real-time channel conditions, resulting in enhanced Spectral Efficiency (SE).

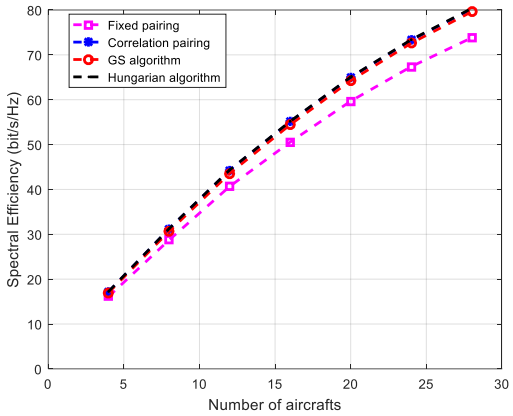

Fig. 3. Spectral efficiency versus number of aircrafts with fixed pairing NOMA and three different pairing algorithms (GS, Hungarian, and correlation-based) with M = 100, ZF beamforming.

Fig. 3 demonstrates the impact of increasing the number of CTGS antennas. With more CTGS antennas, allowing for the transmission of multiple data streams simultaneously, the SE increases. Comparing this result with Fig. 2, we observe that with 36 CTGS antennas and 24 aircrafts, the SE is 56.29 b/s/Hz. However, with 100 CTGS antennas and the same number of aircrafts, the SE rises to 73.4 b/s/Hz.

Fig. 4 depicts the correlation between complexity and the number of aircrafts at a specific number of CTGS antennas. As the number of users increases, the complexity of the three algorithms also rises. The GS technique exhibits the lowest complexity, while correlation-based pairing demonstrates the highest complexity. This difference in complexity is attributed to the formulas discussed in Section III.

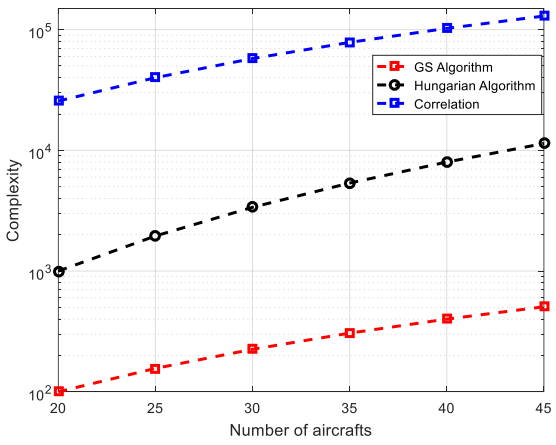

Fig. 4. Aircrafts number versus complexity, using M = 64 CTGS antennas.

Fig. 5 illustrates how complexity changes as the number of CTGS antennas increases. Correlation-based pairing complexity grows linearly with M, whereas the complexity of the Hungarian and the GS algorithms remains constant regarding M. This distinction in complexity arises from the formulas discussed in Section III.

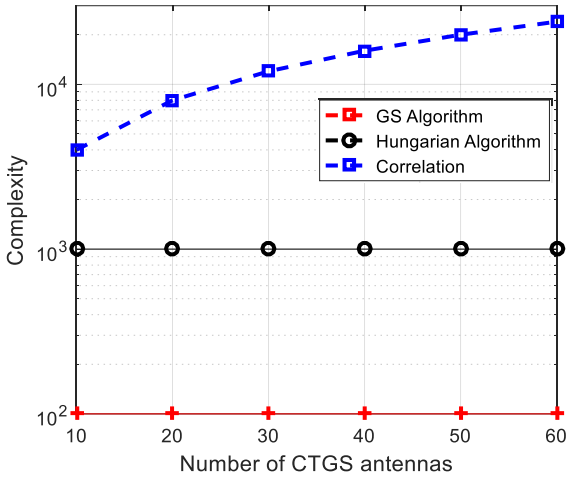

Fig. 5. Complexity vs CTGS antennas number for N = 20 aircrafts.

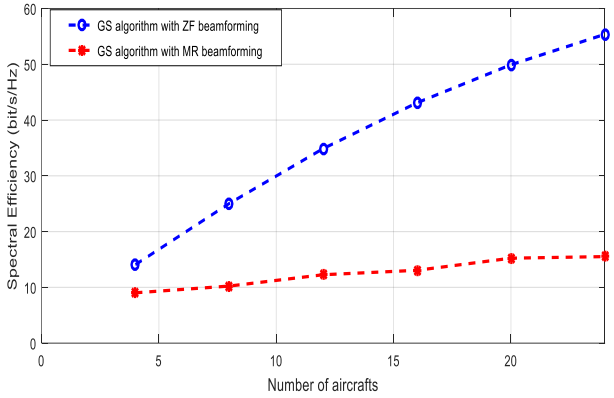

Fig. 6. Spectral efficiency versus the number of aircrafts using the GS algorithm with M = 36, ZF beamforming, and MR beamforming

All previous results were evaluated by employing ZF beamforming. The performance of the MR beamforming technique is shown in Fig. 6. The SE achieved by MR beamforming is lower than that for ZF beamforming, which is due to the fact that ZF beamforming focuses on minimization of inter-user interference.

IV. Conclusion and Future Work

The dedicated spectrum for aeronautical communication has become increasingly congested due to the daily increase in air traffic, so we need to propose different solutions to maximize the capacity of aeronautical communications system. One of these solutions we introduced in our research is using NOMA with massive MIMO. In our work, we aim to maximize the spectral efficiency (SE) of massive MIMO NOMA in aeronautical communication by choosing the optimum NOMA pairs. We employed pairing algorithms like the GS, Hungarian, and correlation-based algorithms with different beamforming techniques such as Zero-Forcing (ZF) and Maximum Ratio (MR). The results show a sufficient maximization of SE using pairing algorithms (GS, Hungarian, and correlation-based) compared to the fixed paring NOMA such as for the number of aircrafts 24 with 100 CTGS antennas the three pairing algorithms provide SE 73.28 b/s/Hz. In contrast, the fixed pairing provides SE 67.38 b/s/Hz. Also, results show that the ZF beamforming technique performs better than the MR beamforming technique. We suggest, as future work, conducting field trials or experiments to confirm the practical viability of the proposed approach. Additionally, we recommend studying complexity with consideration of accuracy for greater reliability.

Conflict of Interest

The authors declare no conflict of interest.

Author Contributions

Amir conducted mathematical analysis, developed the system model, and performed MATLAB simulations. Ahmed and Ihab reviewed the model and analyzed the simulation results. Amir drafted the paper, which was subsequently reviewed by Ihab and Ahmed. Ihab provided the final review and revisions to produce the final version of the paper, all authors have contributed to this work. Amir and Ahmed proposed the idea, which was then formalized in its final version by Ihab. All authors have approved the final version of the manuscript.

References

[1] N. Agrawal, S. J. Darak, and F. Bader, "Spectral coexistence of LDACS and DME: Analysis via hardware software co-design in presence of real channels and RF impairments," *IEEE Trans Veh Technol*, vol. 69, no. 9, pp. 9837–9848, 2020.

[2] M. Schnell, U. Epple, D. Shutin, and N. Schneckenburger, "LDACS: Future aeronautical communications for air-traffic management," *IEEE Communications Magazine*, vol. 52, no. 5, pp. 104–110, 2014.

[3] ICAO/AMCP. Future Aeronautical Mobile Communications Scenario—Report on Agenda Item 2, Appendix a, 8th Meeting of the Aeronautical Mobile Communications Panel (Contribution), [Online]. Available: http://www.icao.int/safety/acp/Inactive%20working%20groups%20library/ AMCP%208/AMCP866-ycr2A.pdf

[4] G. G. E. Leonardo and O. T. J. Eduardo, "VHF data link communications to provide air traffic services in Colombia," in *Proc. 2012 IEEE/AIAA 31st Digital Avionics Systems Conference (DASC)*, IEEE, 2012, p. 5E2-1.

[5] Å. Svensson, U. Ohlander, and J. Lundberg, "Design implications for teamwork in ATC," *Cognition, Technology and Work*, vol. 22, no. 2, pp. 409–426, 2020.

[6] K. V. D. Boogaard, "Agenda item 2: Future air/ground data link systems — The IATA position on the use of 8.33 kHz," *Ground Data Link Systems—The IATA Position on the Use of*, vol. 8, 2003.

[7] R. Jain, F. Templin, and K. S. Yin, "Analysis of L-band digital aeronautical communication systems: L-DACS1 and L-DACS2," in *Proc. 2011 Aerospace Conference*, IEEE, 2011, pp. 1–10.

[8] H. Jamal and D. W. Matolak, "FBMC and L-DACS performance for future air-to-ground communication systems," *IEEE Trans Veh Technol*, vol. 66, no. 6, pp. 5043–5055, 2016.

[9] E. Abd-Elaty, A. Zekry, S. El-Agooz, and A. M. Helaly, "Cognitive radio techniques for utilizing the primary L-band distance measuring equipment for aeronautical communications," *IEEE Access*, vol. 8, pp. 124812–124823, 2020.

[10] L. Wang, M. Liu, J. Zhang, and D. Li, "Adaptive threshold energy detection spectrum sensing method for L-band digital aeronautical

communication system," *Security and Communication Networks*, vol. 2022, 2022.
[11] A. S. Marcano and H. L. Christiansen, "Impact of NOMA on network capacity dimensioning for 5G HetNets," *IEEE Access*, vol. 6, pp. 13587–13603, 2018.
[12] K. Senel, H. V. Cheng, E. Björnson, and E. G. Larsson, "What role can NOMA play in massive MIMO?" *IEEE J Sel Top Signal Process*, vol. 13, no. 3, pp. 597–611, 2019.
[13] T. Parfait, Y. Kuang, and K. Jerry, "Performance analysis and comparison of ZF and MRT based downlink massive MIMO systems," in *Proc. 2014 sixth international conference on ubiquitous and future networks (ICUFN)*, IEEE, 2014, pp. 383–388.
[14] E. Pakdeejit, "Linear precoding performance of massive MU-MIMO downlink system," 2013.
[15] D. Gale and L. S. Shapley, "College admissions and the stability of marriage," *The American Mathematical Monthly*, vol. 69, no. 1, pp. 9–15, 1962.
[16] Gale-Shapley algorithm. [Online]. Available: https://towardsdatascience.com/gale-shapley-algorithm-simply-explained-caa344e643c2
[17] A. S. Marcano and H. L. Christiansen, "Impact of NOMA on network capacity dimensioning for 5G HetNets," *IEEE Access*, vol. 6, pp. 13587–13603, 2018.
[18] Hungarian maximum matching algorithm. [Online]. Available: https://brilliant.org/wiki/hungarian-matching/
[19] T. Senni, I. Fernandez-Hernandez, and S. Cancela, "Evaluation of the Hungarian algorithm for optimal transmission of the Galileo HAS message from multiple satellites," in *Proc. 2022 International Conference on Localization and GNSS (ICL-GNSS)*, IEEE, 2022, pp. 1–5.
[20] A. Cseh, "Complexity, and algorithms in matching problems under preferences," Technische Universitaet Berlin (Germany), 2016.
[21] R. J. Kelly and D. R. Cusick, "Distance measuring equipment and its evolving role in aviation," *Advances in Electronics and Electron Physics*, vol. 68, 1986.
[22] Y. Ishiguro, K. Yoshii, and S. Shimamoto, "Performance evaluation of multiple access scheme applying NOMA for ADS-B," in *Proc. 2022 IEEE/AIAA 41st Digital Avionics Systems Conference (DASC)*, IEEE, 2022, pp. 1–5.